

Central European Journal of Chemistry

Adsorption of nicotinic acid on the surface of nanosized hydroxyapatite and structurally modified hydroxyapatite

Research Article

¹Alexandra-Cristina Dancu, ¹Reka Barabas, ²Erzsebet-Sara Bogya

¹Department of Chemical Engineering and Oxide Material Science, Faculty of Chemistry and Chemical Engineering, Babes-Bolyai University, Cluj-Napoca, Romania

²Department of Physical-Chemistry, Faculty of Chemistry and Chemical Engineering, Babes-Bolyai University, Cluj-Napoca, Romania

Received 7 November 2010; Accepted 20 March 2011

Abstract:In the present paper, hydroxyapatite and structurally modified hydroxyapatite were investigated to establish the best material for nicotinic acid adsorption. Structurally modified hydroxyapatite wa prepared by adding sodium silicate in the reaction medium. The influence of silica concentration, presence of small amounts of metal ions, temperature and initial concentrations of nicotinic acid solutions on the adsorption capacity, were studied. Results indicated that structurally modified hydroxyapatite doped with copper adsorbed the highest amount of nicotinic acid. For this material the adsorption capacity was 0.232 mg nicotinic acid / g material, at an initial concentration of 10⁻⁴ M nicotinic acid. For all types of materials, best results were obtained at 15°C. The amount of nicotinic acid adsorbed increases with the decrease in temperature and with the increase in the initial concentration of nicotinic acid. Adsorption kinetics data were modeled using pseudo-first and pseudo-second order models while the interference due to diffusion was analyzed with intraparticle diffusion model. The results indicate that pseudo-second order model best describes the adsorption kinetics data, indicating the formation of chemical bonding.

The materials used in this study were characterized by the following methods: IR, Coulter Counter analyzer, Scanning Electron Microscope and BET

Keywords: Hydroxyapatite • Silica addition • Nicotinic acid • Adsorption efficiency

© Versita Sp. z o.o.

1. Introduction

Hydroxyapatite (HAP) is a mineral form of calcium apatite with the formula $\text{Ca}_5(\text{PO}_4)_3(\text{OH})$, but is usually written with the formula $\text{Ca}_{10}(\text{PO}_4)_6(\text{OH})_2$ to suggest that the crystal unit cell comprises two entities. Hydroxyapatite is the major component of bones and teeth [1] and is regarded as an important material for implants due to his high biocompatibility with biological systems [2]. HAP can develop tight bonding with bone tissue, exhibits osteoconductive behavior and has no adverse effects on the human organism [3-7].

There are several methods to prepare hydroxyapatite [5,8,9]: wet chemical procedures, hydrothermal treatment, dry processes (solid-state reactions) and hydrolysis. The

type of preparation method has a great influence on the specific surface, crystallinity, stoichiometry and powder morphology.

Hydroxyapatite is widely used in medicine and dentistry. In recent years it has been used principally as bone substitutes or as coating material for prosthesis in the field of medicine [10]. The surface of calcium phosphate is transformed into natural apatite when they are implanted. Other applications of hydroxyapatite are as column packing material for chromatography to separate proteins and enzymes [11-16] adsorbent material for organic acids with small molecular weight, polysaccharides [17], medical substances [18,19]. Hydroxyapatite columns are used for double-strand (ds) DNA and single-strand (ss) DNA separation, an operation desired for DNA analysis [20].

HAP is also used for the removal of toxic metals from wastewaters. These metals, such as Pb, Cd, Cu, Zn, Hg, Cr and Ni are the main contaminants of waters and soils. The main sources of these elements are metal plating industries, abandoned disposal sites and mining industries [21]. Hydroxyapatite has the ability to bind these metal ions from aqueous solutions [22-27]. Many mechanisms have been proposed to describe this process: ion exchange [28,29], surface complexations [28,30], substitution of Ca in HAP by metals during coprecipitation [28,31], dissolution of HAP and precipitation of metal phosphates [28,32]. The sorption of cations on HAP depends on factors such as pH, contact time, initial metal concentration and presence of common competing cations [33].

Hydroxyapatite could also be used for drug delivery in organisms. Drugs administered systematically are absorbed into the blood stream and distributed throughout the host patient via the circulatory system, which can result in bacterial resistance [34-37]. When administered locally, they limit the adverse effect of systemic administration and there is a higher concentration of medication reaching the targeted site [34].

Coatings, particles, porous granules and beads of HAP have been investigated as carriers for different drugs such as antibiotics (gentamicine, doxycycline, minocycline, ampicilin, etc.) and growth factors [38-41]. In this study, nicotinic acid was used as adsorbate. Nicotinic acid (NA) is a B-vitamin, with the formula $C_6H_5NO_2$. In 1955, it was discovered that nicotinic acid, in large doses (>500 mg) lowers cholesterol [42]. It then became the first widely used treatment for dyslipidemia. Nicotinic acid lowers low-density lipoprotein-cholesterol (LDL-C), triglyceride and lipoprotein, it raises the level of high-density lipoprotein-cholesterol (HDL-C) [43]. It was the first drug shown to prevent cardiovascular disease [441]

Ingestion of nicotinic acid by healthy people results in a vasodilatory response. NA induces vasodilatation by stimulating the release of prostaglandins, in particular prostaglandin D2 (PGD2) from the skin. PGD2 stimulates adenylyl cyclase activity in capillary endothelial cells causing vasodilatation [45-47].

2. Experimental Procedure

2.1 Material preparation

2.1.1. Synthesis of hydroxyapatite

To prepare hydroxyapatite, silica-substituted hydroxyapatite and silica-substituted hydroxyapatite doped with copper were used. To prepare hydroxyapatite,

a wet-chemical procedure was used. This procedure involves HAP precipitation by mixing aqueous solutions that contains Ca²⁺ and PO₄³⁻ at pH>9. As a source of Ca²⁺ ions, calcium nitrate solution of 0.5 mol L⁻¹ was used and as PO₄³⁻ ion source diammonium phosphate solution of 0.3 mol L⁻¹ was used. The pH was adjusted using 25% ammonia solution. All the solutions were procured from Merck, Germany. The reaction that occurs is:

$$10Ca(NO_3)_2 + 6(NH_4)_2HPO_4 + 8NH_4OH =$$

= $Ca_{10}(PO_4)_8(OH)_2 + 20NH_4NO_3 + 6H_2O$

Calcium nitrate and a part of ammonia were added to a reactor and stirred. The rest of the ammonia and the diammonium phosphate were slowly added to the above solution of calcium nitrate and ammonia. and reaction continued for 20 hours. The pH was kept between 9 and 9.5 using ammonia and the temperature at 20°C.

After 20 hours, the precipitate was washed, filtered and the filtrate was dried for24 hours at 105°C in an oven.

2.1.2. Synthesis of structurally modified hydroxyapatite

For structurally modified hydroxyapatite the preparation method was the same, with the difference that sodium silicate was added with diammoniacal phosphate and ammonia to the preparation mixture. The silica forms a gel that upon drying and calcinations results in a porus structure of hydroxyapatite. The reaction was carried out for 8 hours (instead of 20 hours as in the case of HAP) and monitored using X-ray diffractograms that showed formation of hydroxyapatite.

Two types of silica-modified hydroxyapatite were prepared: with 5wt% and 10wt% silica.

The mechanism that describes the substitution of a phosphate group by a silicate group is [48]:

$$Ca_{10}(PO_4)_6(OH)_2 + xSiO_4^{4-} \rightarrow Ca_{10}(PO_4)_{6-x}(SiO_4)_x(OH)_{2-x} + xPO_4^{3-} + xOH^{-}$$

2.1.3. Synthesis of HAP doped with copper

To prepare *hydroxyapatite doped with copper*, silica substituted hydroxyapatite was added to a a 10⁻³ M Cu²⁺ solution.

2.2 Material characterization

The studied materials were: non-calcined hydroxyapatite, HAP-Si 5wt%, HAP-Si 10wt% Si and HAP-Si 10wt% Si doped with copper. These materials were characterized using different physico-chemical methods.

Infrared spectrum was obtained with a Jasco FT/IR-615 spectrophotometer; the characteristic vibrations of the compounds were identified. All materials for spectral

analysis were prepared as KBr pellets. Coulter Counter analyzer from Shimadzu SALD-7101 was used for particle size distribution was determined.

Jeol 1010, Scanning Electron Microscope, was used to determine the structure of the materials. The specific surface and porosity, two important characteristics to define a material, were determined by the N_2 adsorption – desorption isotherms using BET analyzer, model QSURF M_3 , work domain 0,015-2000 m^2 g^{-1} .

Nicotinic acid solution absorbance was determined using UV-Vis spectroscopy, with a Jasco V-650 spectrophotometer.

2.3 Nicotinic acid adsorption measurements

For all the experiments nicotinic acid solutions with a concentration between 5×10⁻⁵ and 2.5×10⁻⁴ M were used. The calibration curve was obtained by plotting the absorbance of these solutions versus the concentration in the 220 and 280 nm wavelength region. The experiments were carried out in 25 mL balloons, in a FALC FA-90 thermostat, under continuous stirring provided by a FALC FA-20 magnetic stirrer. The experiments were repeated twice. Double-distilled water was used to prepare nicotinic acid solutions.

For each experiment 0.2 g material and 10 mL nicotinic acid solution of different concentrations were used. After stirring and filtration the absorbance of nicotinic acid in solution was measured. Based on the calibration curve, the concentration of nicotinic acid that remained in solution and the amount of nicotinic acid adsorbed on the surface of hydroxyapatite, were determined. The adsorption process efficiency and the adsorption capacity were also investigated.

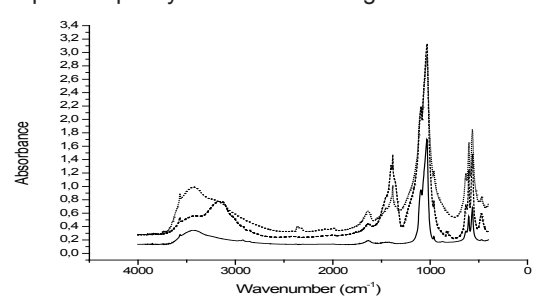


Figure 1. IR spectra of HAP (solid line), HAP-Si 5wt% Si (dotted line) and HAP-Si 10wt% Si (dashed line)

Table 1. Specific surfaces of HAP, HAP-Si 5wt% and HAP-Si 10wt% Si

Material	Specific surface (m² g-1)
HAP<45 nm	73.68
HAP-Si 5% <45 nm	89.79
HAP-Si 10% >45 nm	124.37

3. Results and Discussion

3.1 Material characterization

Fig. 1 shows the Infrared spectra that were obtained:

Gibson *et al.* [48] stated that the incorporation of silicon in the HAP lattice, even in small amounts, resulted in an increase of the PO $_4^{3-}$ tetrahedral distortion. Silicon substitution seem to affect the FTIR spectra of HAP, in particular the P—O vibrational bands. The distortion is caused by the stretching vibrations assigned to the Si—O—Si bonds that should appear in the range of 950–1200 cm $^{-1}$ but due to the presence of the phosphate groups, these peaks cannot be observed. Isolated Si—OH groups on silica show a sharp band at 3750 cm $^{-1}$. The peak at 1384 cm $^{-1}$ appeared due to a small amount of inorganic nitrate present in the sample [49].

Coulter Counter was used to determine the particle size, in suspension. For non-modified hydroxyapatite and HAP-Si 10wt% silica the average particle size was 15 nm, while for HAP-Si with 5wt% silica the average particle size was 800 nm.

SEM analysis shows the morphological differences of the materials. (Figs. 2a-2f).

HAP presented spherical granulation compared to the materials that contained silica. HAP-Si has a compact structure. For HAP-Si doped with copper, at higher resolution, a finer distribution of the particles on the surface of the material can be seen which is due to the bond between copper ions and hydroxyl function of hydroxyapatite [50].

Using the method of Brunauer, Emmett and Teller the specific surface of hydroxyapatite and structurally modified hydroxyapatite was determined. The specific surfaces of HAP, HAP-Si 5wt%, HAP-Si 10wt% Siare presented in Table 1.

It can be concluded that structurally modified hydroxyapatite has a higher specific surface than non-modified hydroxyapatite. This could be explained by the fact that silica forms a water enriched gel, which after a process of drying and calcinations loses water, resulting in micro- and macro-pores.

3.2 Nicotinic acid adsorption measurements

The influence of material, nicotinic acid solutions temperature and concentration were studied.

The absorbance of nicotinic acid solution gave the spectrum seen in Fig. 3.

According to Fig. 3 nicotinic acid solution has an absorption maximum at 261 nm.

The first parameter studied was the *type of the material*. As mentioned before, in this experiment

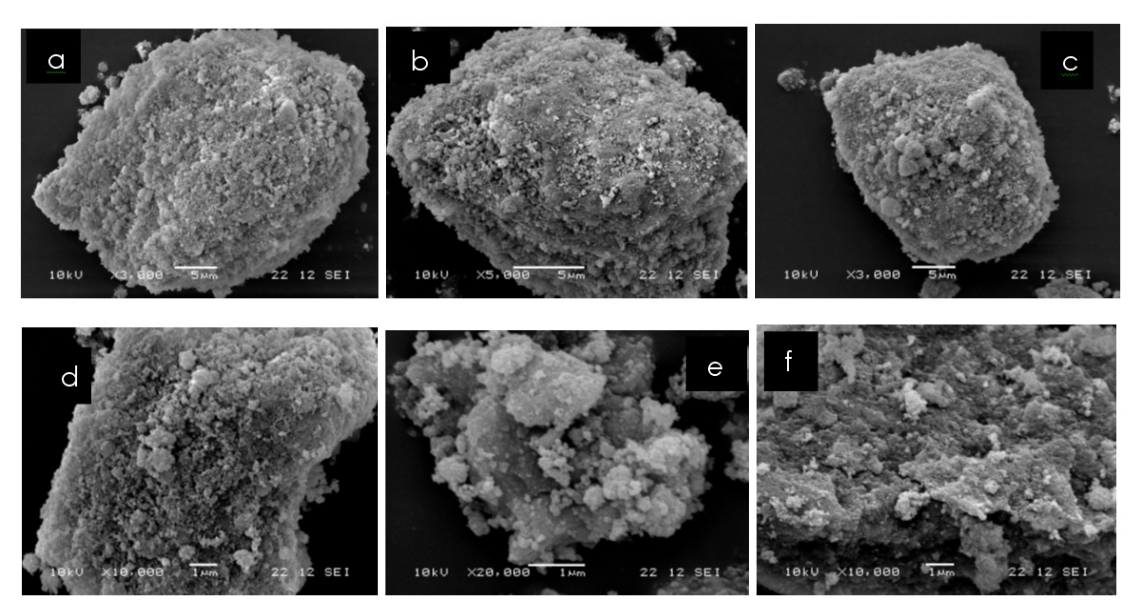


Figure 2. Scanning electron microscope for HAP (a,d), HAP-Si (b,e) and HAP-Si doped with copper (c,f)

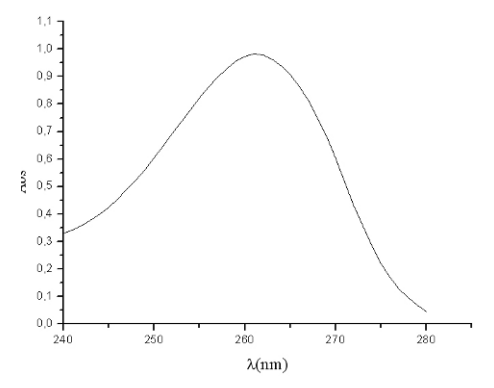


Figure 3. The absorbance of nicotinic acid solution 2.5×10-4 M

four types of materials were used: non-calcined hydroxyapatite, HAP-Si 5 wt%, HAP-Si 10 wt% Si and HAP-Si 10wt% Si doped with copper. In all these experiments a 10^{-4} M nicotinic acid solution was used and the temperature was maintained at 20° C.

The adsorption efficiency was calculated with the formula:

$$\eta = \frac{c_0 - c_i}{c_0} \%,$$

where, c_0 is the initial concentration of nicotinic acid solutions and c_i is the concentration of nicotinic acid solutions at different periods of time. The *adsorption capacity* was calculated using the formula:

$$Q_a = \frac{m_{ads}}{m},$$

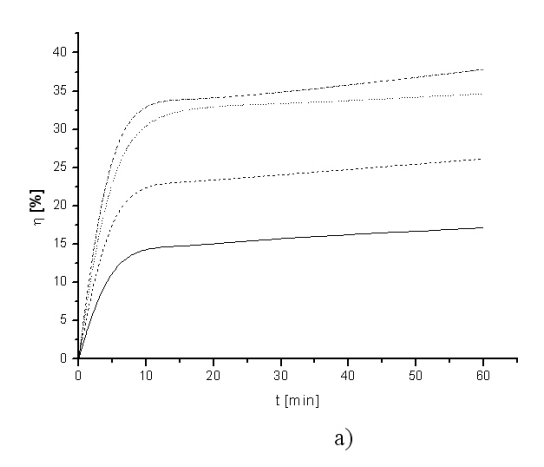
where, m_{ads} is the adsorbed amount of nicotinic acid (mg) at a specific time and m the quantity of the material on which it was adsorbed (g).

The results are presented in Figs. 4a and 4b.

From these figures it can be observed that structurally modified hydroxyapatite adsorbed more nicotinic acid than un-modified hydroxyapatite. For the materials studied, the quantity of nicotinic acid adsorbed was proportional to the percentage of silica. The material which had the highest adsorption efficiency was HAP-Si 10 wt% Si doped with copper. That is because HAP-Si 10 wt% Si has the highest specific surface and copper may form chemical bounds with nicotinic acid or may create active sites on the surface of hydroxyapatite, that facilitate the adsorption process. Further studies have to be done in order to determine the processes that occur on the surface of hydroxyapatite doped with copper. The adsorption capacity of this material was 0.232 mg nicotinic acid / g hydroxyapatite, at a concentration of nicotinic acid 10-4 M. Studies with nicotinic acid solutions 10-2 M were also done, but using these solutions the suprasaturation was reached from the beginning. It was not useful to study the kinetics of the adsorption process at such high concentrations, but from the data the maximum adsorption capacity can be determined. The maximum adsorption capacity of noncalcined hydroxyapatite was 12.29 mg nicotinic acid / g of hydroxyapatite.

In the present paper, the influence of temperature over the adsorption process was also studied. The experiments were carried out at three temperatures: 15, 20 and 30°C. These temperatures were varied for all four types of materials. The results are shown in Fig. 5.

For all four material types it cwas noted that the best results were obtained at 15°C. The amount of nicotinic acid adsorbed increases with the decrease in



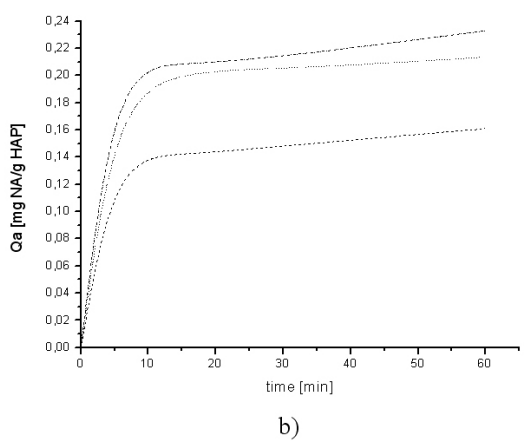


Figure 4. The adsorption efficiency (a) and capacity (b) of HAP (solid line), HAP-Si 5 wt% Si (dashed line), HAP-Si 10 wt% Si (short dotted line) and HAP-Si 10 wt% Si doped with copper (dash dotted line)

Table 2. Correlation coefficients and rate constants for the kinetic models at 15, 20 and 30°C

т	Pseudo-first order kinetic model		Pseudo-second order kinetic model			
	k₁/min	\mathbf{q}_{e}	R²	k ₂	\mathbf{q}_{e}	R²
(°C)	(L min ⁻¹)	(mg g ⁻¹)		(min g mg ⁻¹)	(mg g ⁻¹)	
15	8.41×10 ⁻²	13.32	0.7695	6.83	0.15	0.9994
20	2.20×10 ⁻²	12.63	0.5769	9.22	0.11	0.9979
30	1.75×10 ⁻²	12.10	0.7415	4.44	0.10	0.9991

temperature. An explanation for this observation could be that with increasing temperatures the solubility of nicotinic acid also increases, and thus being desorbed from the hydroxyapatite's surface.

The effect of *initial concentration of nicotinic acid solutions* on adsorption was also studied. The adsorption efficiency was calculated for non-calcined hydroxyapatite for two concentrations of nicotinic acid solutions: 10^{-4} M and 2×10^{-4} M, at three temperatures. The results are presented in Fig. 6.

It is possible that the amount of nicotinic acid adsorbed depends on the initial solution concentrations. The concentration of 2×10^4 M gave the best results.

3.3 Adsorption kinetics

A study of adsorption kinetics is important because it provides information about the mechanism of adsorption, which is important for the efficiency of the process.

In order to analyze the adsorption kinetics of nicotinic acid, the pseudo-first and pseudo-second order model were applied to data.

The pseudo-first order equation, or Lagergren equation, for reversible reactions, is represented as [51]:

$$\frac{dq_t}{dt} = k1 \cdot (q_e - q_t) \tag{1}$$

where q_e and q_t are the amounts of nicotinic acid adsorbed on the hydroxyapatite at the equilibrium and at time t, respectively (mg g^{-1}) and k_1 is the rate constant of pseudo-first order (L min⁻¹). Integrating and applying the boundary condition t=0 and q_t =0 to t=t and q_e = q_t , Eq. 1 takes the form:

$$\ln(q_e - q_t) = \ln q_e - k1 \cdot t \tag{2}$$

This equation is applicable if the reaction is irreversible. A straight line of $ln(q_e-q_t)$ versus t indicates the application of the pseudo-first order kinetic model. The rate k_1 was obtained from the slope of the linear plot.

The sorption data were analyzed using the pseudosecond order model described by the following equation [52,53]:

$$\frac{dq_t}{dt} = k2 \cdot (q_e - q_t)^2 \tag{3}$$

where, k2 is the second order reaction rate equilibrium constant (min g mg⁻¹). Integrating and applying the boundary condition t=0 and qt=0 to t=t and qe=qt, Eq. 3 takes the form:

$$\frac{1}{q_t} = \frac{1}{k2 \cdot q_e^2} + \frac{t}{q_e} \tag{4}$$

If the pseudo-second order model is applicable, the plot of t/qt *versus* t should give a linear relation from which ge and k2 can be determined.

Fig. 7 presents the plots for the adsorption of nicotinic acid using the pseudo-first order kinetic model (a) and pseudo-second order kinetic model (b).

Correlation coefficients and kinetic parameters are presented in Table 2. The values of rate constants and the equilibrium adsorption capacity determined with the pseudo-first order and pseudo-second order kinetic models are also presented. The results presented in Table 2 and graphical representations showed that the pseudo-second order kinetic model provided the best correlation with experimental data.

In the case of Lagergren equation, the values of equilibrium adsorption capacity vary an order of magnitude from the real values and from the values obtained using the pseudo-second order kinetic model. The correlation coefficients are very low. All of these things indicate that the adsorption of nicotinic acid on the surface of hydroxyapatite follows the pseudo-second order kinetic model. When pseudo-second

order kinetic model provides the best correlation of the data, the sorption system is not a first order reaction, based on the assumption that the rate limiting step may be chemical sorption or chemisorptions involving valency forces through sharing or exchange of electrons between sorbent and sorbate [54].

The values of rate constants determined with the pseudo-second order kinetic model versus time were represented to calculate the heat of adsorption process [54]. The values obtained are presented in Table 3. These values are negative therefore, suggest that the process of nicotinic acid adsorption is an exothermic one.

Table 3. The heat of adsorption determined using the rate constants calculated from the pseudo-second order kinetic model

Material	ΔH (kJ mol ⁻¹)	
HAP	-17.9	
HAP-Si 5 wt%	-17.4	
HAP-Si 10 wt%	-11.8	
HAP-Si 10 wt% + Cu	-8.1	

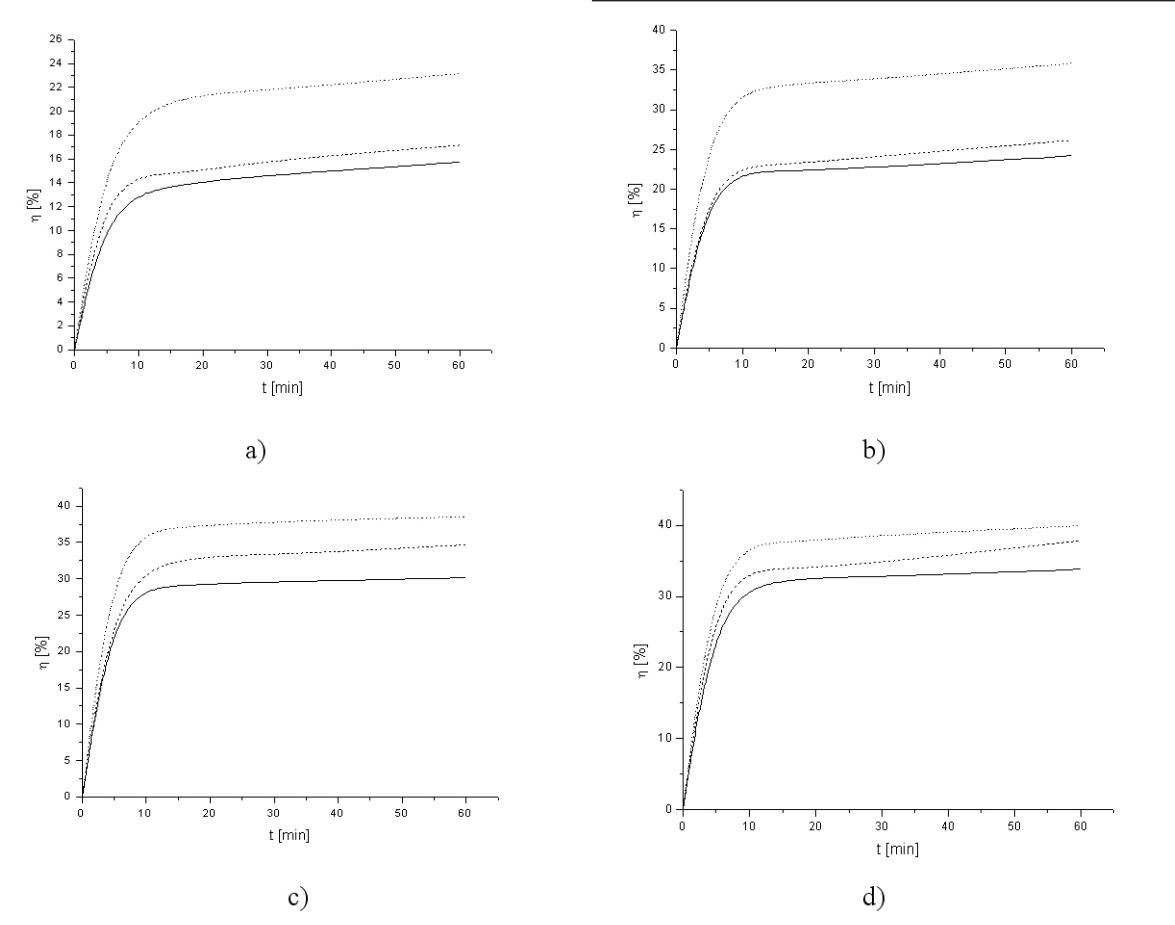


Figure 5. The adsorption efficiency of HAP (a), HAP-Si 5 wt% (b), HAP-Si 10 wt% Si (c) and HAP-Si 10 wt% Si doped with copper(d) at 15°C (short dotted line), 20°C (dashed line) and 30°C (solid line)

The mechanism of sorption is either film diffusion controlled or particle diffusion controlled. Before adsorption occurs, several diffusion processes takes place. The sorbate will have to diffuse through the bulk of the solution to the film surrounding the adsorbent and then into the micro pores and macro pores of the adsorbent. When the last one is the rate limiting step, the sorption mechanism is intraparticle diffusion controlled.

A model for intraparticle diffusion was developed in 1980:

$$q_t = Xi + k3 \cdot t^{0.5} \tag{5}$$

where k3 is intraparticle diffusion rate constant. Values of Xi give an idea about the thickness of the boundary layer; the larger intercept the greater is the boundary layer effect. Fig. 8 represents the plot for the adsorption of nicotinic acid using intraparticle diffusion model.

The values of the diffusion rate constant and the boundary layer thickness are given in Table 4. Low values of the regression coefficients indicate that the model does not describe the adsorbtion process, and confirms that the adsorption of the nicotinic acid on hydroxyapatite is not intraparticle diffusion controlled.

Table 4. Parameters of intraparticle diffusion model for hydroxyapatite

Temperature	Intraparticle diffusion model			
(°C)	k3 (mol L ⁻¹ min ^{-0.5})	R²	Xi	
15	0.0006	0.8415	0.0102	
20	0.0003	0.9240	0.0081	
30	0.0004	0.9701	0.0069	

Table 5. Isotherms and their linear form

Isotherm		Linear form	
Freundlich	$q_e = K_F C_e^{1/n}$	$log(q_e) = log(K_F) + \frac{1}{n}log(C_e)$	
Langmuir-1		$\frac{C_e}{q_e} = \frac{1}{q_m}C_e + \frac{1}{K_a q_m}$	
Langmuir-2	$q_e = \frac{q_m K_a C_e}{1 + K_a C_e}$	$\frac{1}{q_e} = (\frac{1}{K_a q_m}) \frac{1}{C_e} + \frac{1}{q_m}$	
Langmuir-3		$q_e = q_m - (\frac{1}{K_a}) \frac{q_e}{C_e}$	
Langmuir-4		$\frac{q_e}{C_e} = K_a q_m - K_a q_e$	

3.4 Adsorption isotherms

Several mathematical models have been developed to quantitatively express the relationship between the extent of sorption and the residual solute concentration. The most widely used models are the Langmuir and Freundlich adsorption isotherm models. The Langmuir adsorption isotherm describes quantitatively the build up of a layer of molecules on an adsorbent surface as a function of the concentration of the adsorbent material in the liquid in which it is in contact. In a modified form it can also describe a bi-layer deposition. The shape of the isotherm is a gradual positive curve that flattens to a constant value. The Freundlich isotherm curve in the opposite way and is exponential in form. It often represents an initial surface adsorption followed by a condensation effect resulting from extremely strong solute-solute interaction. Table 5 presents these isotherms and their linear forms [55].

Applicability of the isotherms using the data presented in Table 6.

Table 6. Equilibrium concentrations and equilibrium adsorption capacity for different nicotinic acid initial concentrations at T=273 K

C _{initial}	C _{ads} (mg L ⁻¹)	Q _{ads} (mg g ⁻¹)
10-3	4.8×10 ⁻⁵	4.8×10 ⁻²
8×10-4	4.5×10 ⁻⁵	4.5×10 ⁻²
6×10-4	2.8×10 ⁻⁵	2.8×10 ⁻²
4×10-4	2.7×10 ⁻⁵	2.7×10 ⁻²
2×10-4	1.1×10 ⁻⁵	1.1×10 ⁻²
10-4	3.3×10 ⁻⁶	3.3×10 ⁻³
8×10 ⁻⁵	2.0×10 ⁻⁶	2.0×10 ⁻²

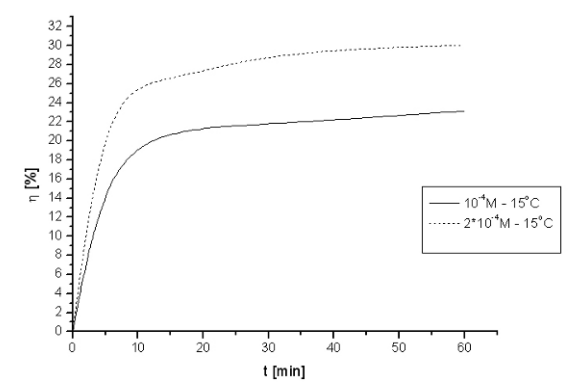
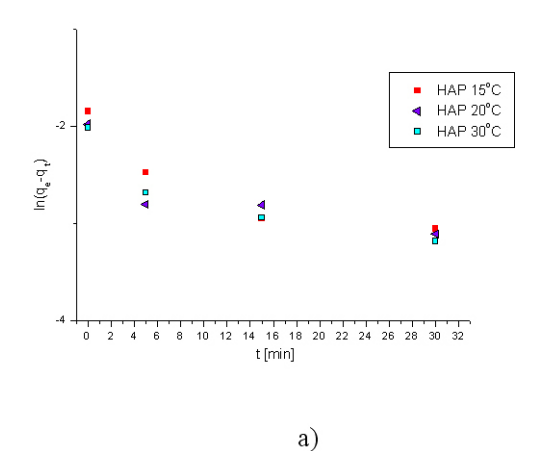


Figure 6. The adsorption efficiency for HAP in nicotinic acid solutions 10⁴ M (solid line) and 2×10⁻⁴ M (dashed line) at 15°C.



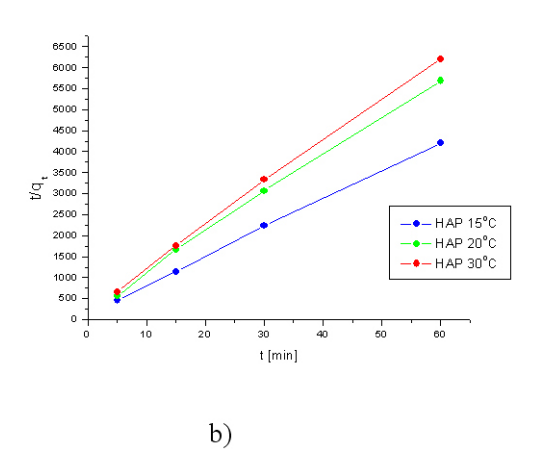


Figure 7. The applicability of the pseudo-first order kinetic model (a) and pseudo-second order kinetic model (b) to nicotinic acid adsorption on hydroxyapatite

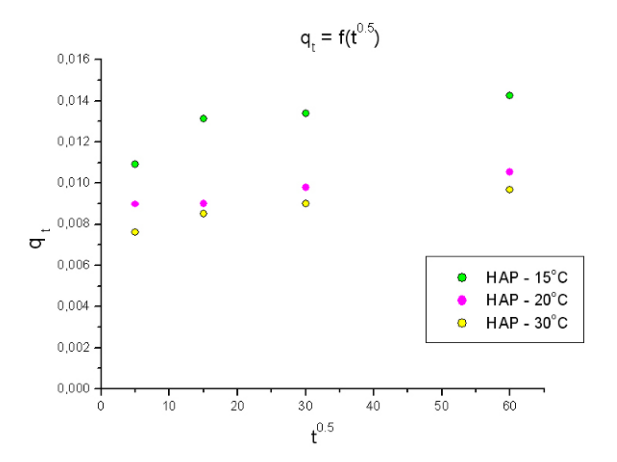


Figure 8. The applicability of intraparticle diffusion model to nicotinic acid adsorption on hydroxyapatite

Table 7. Parameters obtained using Freundlich and Langmuir isotherms for the adsorption of nicotinic acid solutions on the surface of hydroxyapatite

Isotherm	Parameters obtained	Results
	q _m (mg g ⁻¹)	2.6
Langmuir-2	K _a (L mg⁻¹)	5.4×10 ⁴
	R ²	0.86
	K _F (mg g ⁻¹)(L mg ⁻¹) ^{1/n}	4.6
Freundlich	1/n	3.3
	\mathbb{R}^2	0.89

Good correlation data were obtained using Freundlich isotherm and the linearization Langmuir 2. The parameters obtained are presented in Table 7. For Freundlich linearization the correlation coefficient is higher, therefore Freundlich isotherm

is more compatible then the Langmuirone for the equilibrium description. This model describes the systems with a low degree of surface occupation.

4. Conclusions

Hydroxyapatite was prepared using a wet chemical procedure and structurally modified hydroxyapatite was synthesized – with good reproductibility – by adding sodium silicate in the reaction medium. The preparation of silica substituted hydroxyapatite by the addition of natrium silicate as silica source in wet chemical synthesis presented a novelty in the reaction. This method has not been described in the literature before. HAP-Si 5 wt% Si had a larger particle size. Specific surface was seen to increase in the order: HAP, HAP-Si 5 wt% Si and HAP-Si 10 wt% Si.

Structurally modified hydroxyapatite has adsorption efficiency higher than non-modified hydroxyapatite. The adsorption efficiency is proportional to the percentage of silica in hydroxyapatite for the interval studied. The efficiency rises with decrease in temperature. The most efficient adsorption was observed in the case of silica-modified hydroxyapatite doped with copper and the highest adsorption capacity was reached at 15°C within the temperature range studied.

The reaction kinetics obeyed pseudo-second order model and the mechanism of adsorption was found to be *via* the formation of chemical bonds between the active centers on the surface of the apatite and nicotinic acid molecules. The intercalation of copper ions in the apatite material increased the adsorption capacity of the material. This can be explained by the formation of additional active centers on the surface of the hydroxyapatite. The calculated adsorption heat, from

the pseudo-second order rate constant, showed that the adsorption process is exothermic, which explains the decrease of adsorption capacity with the increase in temperature.

References

- [1] L.L Hench, J. Am. Ceram. Soc. 74, 1487 (1991)
- [2] W. Suchanek, M. Yoshimura, J. Mater. Res. 13, 94 (1998)
- [3] H. Aoki, Science and medical applications of hydroxyapatite (JAAS, Japan, 1991)
- [4] D.F. Williams, Adv. Mater. Technol. Monitor. 2, 1 (1994)
- [5] V.P. Orlovskii, G.E. Sukhanova, Zh.A. Ezhova, G.V. Rodicheva, Zh. Vses. Khim. o-va. im. D.I. Mendeleeva 36, 683 (1991) (In Russian)
- [6] L.L Hench, Ceramics and Society 101 (1995)
- [7] Yu.D. Tret'yakov, O.A. Brylev, Ross. Khim. Zh. 7(4), 10 (2000) (In Russian)
- [8] W. Cao, L.L. Hench, Ceram. Int. 22, 493 (1996)
- [9] A.J. Monma, J. Ceram. Soc. Jpn, Dent. Res. 8, 97 (1980)
- [10] M.G.S. Murray, J. Wang, C.B. Ponton, P.M. Marquis, J. Mater. Sci 30, 3061 (1995)
- [11] K Kandori, A. Fudo, T. Ishikawa, Phys. Chem. Chem. Phys 2, 2015, (2000)
- [12] A. Tiselius, S. Hjerten, O. Levin, Arch. Biochem. Biophys 65, 132 (1956)
- [13] T. Kawasaki, K. Ikeda, S. Takahashi, Y. Kuboki, Eur. J. Biochem. 155, 249 (1986)
- [14] T. Kawasaki, W. Kobayashi, K. Ikeda, S. Takahashi, H. Monma, Eur. J. Biochem. 157, 291 (1986)
- [15] K. Tomod, H. Ariizumi, T. Nakaji, T. Makino, Colloid Surface B, 76, 226 (2010)
- [16] C. Xu, D. He, L. Zeng, S. Luo, Colloid Surface B, 73, 360 (2009)
- [17] A.S. Gordon, F.K. Millero, Microb. Ecol. 4, 289 (2005)
- [18] A.C. Queiroz, J.D. Santos, F.J. Monteiro, I.R. Gibson, J.C. Knowles, Biomaterials 22, 1393 (2001)
- [19] B. Palazzo, M.C. Sidoti, N. Roveri et all, Mater. Sci. Eng. C-Biomim. 25, 207 (2005)
- [20] W.Y. Chen, M.S. Lin, P.H. Lin, P.S. Tasi, Y. Chang, S. Yamamota, Colloid Surface A 295, 274 (2007)
- [21] C.N. Mulligan, R.N. Yong, B.F. Gibbs, Eng. Geol. 60, 193 (2001)
- [22] D. Marchat, D. Bernache-Assollant, E. Champion, J. Hazard. Mater. 139, 453 (2007)
- [23] T. Suzuki, T. Hatsushika, M. Michihiro, J. Chem. Soc. Faraday Trans. 1, 3605 (1982)
- [24] M. Peld, K. Tonsuaadu, V. Bender, Environ. Sci.

Thermodynamic studies show that the adsorption equilibrium can be described with a higher correlation constant by Freundlich isotherm, a model that describes the systems with a low degree of surface occupation.

- Technol. 38, 5626 (2004)
- [25] A. Corami, S. Mignardi, V. Ferrini, J. Hazard. Mater. 146, 164 (2007)
- [26] A. Yasukawa, T. Yokoyama, K. Kandori, T. Ishikawa, Colloid Surface A 299, 203 (2007)
- [27] R.E. Sheha, J. Colloid Interf. Sci. 310, 18 (2007)
- [28] Y. Xu, F.W. Schwartz, S.J. Traina, Environ. Sci. Technol. 28, 1472 (1994)
- [29] J.A. Gomez del Rio, P.J. Morando, D.S. Cicerone, J. Environ. Manage 71, 169 (2004)
- [30] A.G. Leyva, J. Marrero, P. Smichowski, D. Cicerone, Environ. Sci. Technol. 35, 3669 (2001)
- [31] J. Jeanjean, V. Vincent, M. Fedoroff, J. Solid State Chem. 108, 68 (1994)
- [32] Q.Y Ma, T.J. Logan, S.J. Traina, J.A. Ryan, Environ. Sci. Technol. 28, 1219 (1994)
- [33] I. Smiciklas, A. Onjia, S. Raicevic, D. Janackovic, M. Mitric, J. Hazard. Mater. 152, 876 (2008)
- [34] B.V. Somayaji, U. Jariwala, P. Jayachandran, K. Vidyalakshmi, R.V. Dudhani, J. Periodontol. 69, 409 (1998)
- [35] W.A. Soskolne, P.A. Heasman, J. Periodontol. 68, 32 (1997)
- [36] D. Steinberg, M. Friedman, A. Soskolne, M.N. Sela, J. Periodontol. 61, 393 (1990)
- [37] K. Stoltze, J. Clin. Periodontol. 19, 698 (1992)
- [38] P.S. Gomes, J.D. Santos, M.H. Fernandes, Acta Biomaterialia 4, 630 (2008)
- [39] S. Lepretre, F. Chai, J.C. Hornez, G. Vermet, C. Neut, M. Descamps, H.F. Hildebraud, B. Martel, Biomaterials 30, 6086 (2009)
- [40] Q. Xu, Y. Tanaka, J.T. Czernuszka, Biomaterials 28, 2687 (2007)
- [41] E. Ojewole, I. Mackraj, P. Naidoo, T. Govender, Eur. J. Pharm. Biopharm. 70, 697 (2008)
- [42] R. Altschul, A. Hoffer, J.D. Stephen, Arch. Biochem. 54, 558 (1955)
- [43] C.D. Meyers, V.S. Kamanna, M.L. Kashyap, Curr. Opin. Lipidol. 15, 659 (2004)
- [44] P.L. Canner, K.G. Berge, N.K. Wenger, et all., J. Am. Coll. Cardiol. 8, 1245 (1986)
- [45] R.H. Stern, J.D. Spence, D.J. Freeman, A. Parbtani, Clin. Pharmacol. Ther. 50, 66 (1991)
- [46] J.D. Morrow, J.A. Awad, J.A. Oates, L.J. Roberts, J. Invest. Dermotol. 98, 812 (1992)
- [47] J.D. Morrow, W.G. Parsons, L.J. Roberts,

- Prostaglandins 38, 263 (1989)
- [48] I.R. Gibson, S.M. Best, W. Bonfield, J. Biomed. Mater. Res. 44, 422 (1999)
- [49] P.J Launer, In: R. Anderson, B. Arkles, G.L. Larson (Eds.), Infrared analysis of organosilicon compounds: Spectra-structure correlations. Silicon compounds, register and Review, 4th edition (P.A, Petrarch Systems, Bristol, 1987)
- [50] E. Bogya, R. Barabas, A. Csavdari, V. Dejeu,I. Baldea, Chem. Pap. 63, 568 (2009)
- [51] S. Lagergren, Kungliga Svenska Vetenskapsakademiens, Handlingar 24, 1 (1898)
- [52] F.C. Wu, R.L. Tseng, R.S. Juang, Water Res. 35, 613 (2001)
- [53] P. Antonio, K. Iha, M.E.V. Suarez-Iha, J. Colloid Interf. Sci. 307, 24 (2007)
- [54] Y.S. Ho, G. McKay, Process Biochem. 34, 451 (1999)
- [55] Y.S. Ho, Pol. J. Environ. Stud. 1, 81 (2006)